take place. In all cases no significant anisotropy is observed, indicating that melting is necessary to obtain alignment.

Our method has several advantages over existing techniques. The temperatures and magnetic fields required during sample preparation are relatively modest. The direction of the crystal orientation can be controlled carefully and easily. In addition, because of the relatively rapid cooling rates used during the thermal treatment cycle, the sample production times are significantly shorter than those commonly experienced in melt-texture-growth techniques[7–9]. If the alignment is due to the presence of anisotropic magnetic particles into a liquid, the efficiency of the process will depend on the size and the number of nuclei that are aligned by the field, and consequently on the heating rate, the time and the temperature of the annealing and the cooling rate, all of which govern the grain growth. The process could be adapted for industrial production of textured samples and may prove to be generally applicable to all magnetic substances that have a residual magnetic anisotropy at high temperature. □

Received 17 October 1990; accepted 8 January 1991.

1. Farrel, D. E. *et al. Phys. Rev.* B **36,** 4025–4027 (1987).
2. Livingston, J. D., Hart, H. R. Jr & Wolf, W. P. *J. appl. Phys.* **64,** 5806–5808 (1988).
3. Nakagawa, Y., Yamasaki, H., Obara, H. & Kimura, Y. *Jap. J. appl. Phys.* **28,** L547–L550 (1989).
4. Lees, M. *et al.* in Proc. Int. Conf. '*From Modern Superconductivity Towards Applications*' (ed. Tournier, R. & Suryanarayanan, R.) 49–54 (IITT International Gournay-sur-Marne, 1990).
5. De Rango, P., Lees, M., Lejay, P., Sulpice, A. & Tournier, R. in Proc. Int. Conf. '*From Modern Superconductivity Towards Applications*' (ed. Tournier, R. & Suryanarayanan, R.) 21–26 (IITT International, Gournay-sur-Marne, 1990).
6. Miljak, M., Collin, G. & Hamzic, A. *J. Mag. Mater.* **76 & 77,** 609–611 (1988).
7. Jin, S. *et al. Appl. Phys. Lett.* **52,** 2074–2076 (1988).
8. Salama, K., Selvamanickam, V., Gao, L. & Sun, K. *Appl. Phys. Lett.* **54,** 2352–2354 (1989).
9. Meng, R. L. *et al. Nature* **345,** 326–328 (1990).
10. Schulz, L. G. *J. appl. Phys.* **20,** 1030 (1949).

Estimates of the effect of Southern Ocean iron fertilization on atmospheric CO_2 concentrations

F. Joos*, J. L. Sarmiento† & U. Siegenthaler*

* Physics Institute, University of Bern, CH-3012 Bern, Switzerland
† Atmospheric and Oceanic Sciences Program, Princeton University, Princeton, New Jersey 08544, USA

It has been suggested[1–3] that fertilizing the ocean with iron might offset the continuing increase in atmospheric CO_2 by enhancing the biological uptake of carbon, thereby decreasing the surface-ocean partial pressure of CO_2 and drawing down CO_2 from the atmosphere. Using a box model, we present estimates of the maximum possible effect of iron fertilization, assuming that iron is continuously added to the phosphate-rich waters of the Southern Ocean, which corresponds to 16% of the world ocean surface. We find that after 100 years of fertilization, the atmospheric CO_2 concentration would be 59 p.p.m. below what it would have been with no fertilization, assuming no anthropogenic CO_2 emissions, and 90–107 p.p.m. less when anthropogenic emissions are included in the calculation. Such a large uptake of CO_2 is unlikely to be achieved in practice, owing to a variety of constraints that require further study; the effect of iron fertilization on the ecology of the Southern Ocean also remains to be evaluated. Thus, the most effective and reliable strategy for reducing future increases in atmospheric CO_2 continues to be control of anthropogenic emissions.

A flux of dead biogenic organic matter from the ocean surface continuously transports carbon (and nutrients) to depth and thus influences the surface concentration of total dissolved inorganic carbon (ΣCO_2). Model studies have shown that variations in the efficiency of biological uptake and export of organic carbon in the Southern Ocean, where concentrations of the nutrients P and N are high, can lead to alterations of atmospheric CO_2 in excess of 100 p.p.m.[4–7]. Recently, it has been suggested that biological production in these regions may be limited by a restricted supply of iron[8–11]. Although the hypothesis that iron is the ultimate limiting factor there is controversial[12–14], we adopt it here to obtain upper-limit estimates of the possible reduction in atmospheric CO_2. Because the ratio of iron to carbon incorporated in plants is rather low, between 1:10,000 and 1:100,000[15,16], the amount of iron required to carry out this fertilization is relatively modest: $\sim 10^6$ tons of iron per year assuming that all the iron goes into organic matter. Our model study differs from that of Peng and Broecker[17] in the area fertilized (16% of the world ocean rather than 10%), and in that we include scenarios with anthropogenic CO_2 emissions for which we find that fertilization has a greater effect than when we assume no man-made emissions.

We consider there to be three factors that exert the most important control on the response of atmospheric CO_2 to an

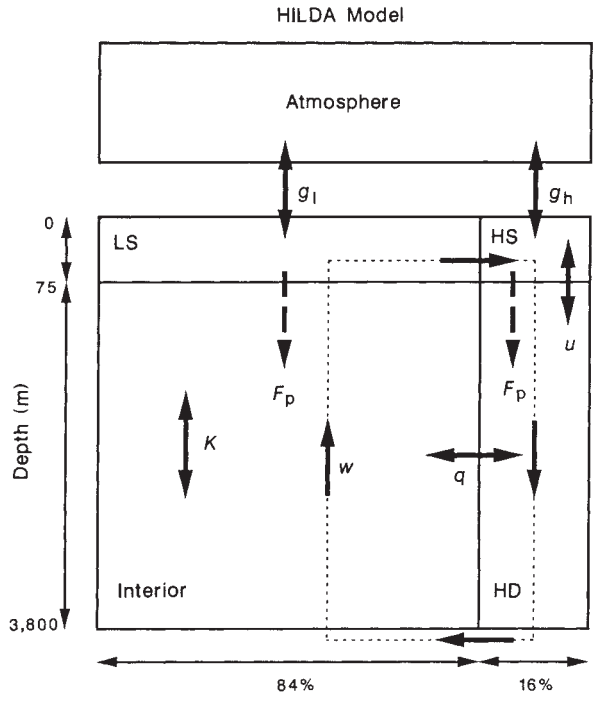

FIG. 1 Structure of the model used for our study, which is based on a model developed by G. Shaffer (personal communication) and one of us (J.L.S.). The ocean interior is resolved by a vertical stack of boxes connected by advection (w) and diffusion (K). The high-latitude regions are simulated by two well-mixed boxes which are connected to each other by mixing (u). The parameter q is a rudimentary representation of the ventilation of the interior oceans by high-latitude waters. The model parameters obtained by fitting bomb and natural ^{14}C are: $K = 465 + 7{,}096 \times \exp(-(z - 75\,m)/253\,m)\ m^2\ yr^{-1}$; $w = 0.44\ m\ yr^{-1}$ (equivalent to $4.24 \times 10^6\ m^3\ s^{-1}$); $u = 38\ m\ yr^{-1}$ ($69.8 \times 10^6\ m^3\ s^{-1}$); $q = 0.00186\ yr^{-1}$ ($79.5 \times 10^6\ m^3\ s^{-1}$); gas-exchange rate ($g_l$, g_h) at 280 p.p.m. = $15.1\ mol\ m^{-2}\ yr^{-1}$; ocean surface area = $3.62 \times 10^{14}\ m^2$; depth of mixed layer = 75 m; average depth of ocean = 3,800 m. We solve conservation equations for the perturbation of phosphate and CO_2 ($c_{pert.} = c_{actual} - c_{unpert.}$) with an initial condition for $c_{pert.}$ of 0 everywhere. The relation between changes of ΣCO_2 and P_{CO_2} is calculated using the equations of Peng *et al.*[24]. The phosphate and carbon removed from the surface high-latitude box are regenerated to the dissolved form in the deep box below (dashed arrows, F_p = perturbation flux of particulate carbon and phosphorus). A small amount of this excess phosphate makes its way through the deep sea to low-latitude surface waters, where it is removed and regenerated below with an exponential scale depth of 1,160 m obtained from a fit to oceanic nutrient data by G. Shaffer and J.L.S. Multiplying the resulting phosphate fluxes by the C:P Redfield ratio (130) gives the corresponding carbon fluxes. LS, low-latitude surface; HS, high-latitude surface; and HD, high-latitude deep boxes.

TABLE 1 Projected changes in atmospheric CO_2 partial pressures resulting from various scenarios beginning in 1990

Scenario*	After 50 years A Unfertilized	After 50 years B Fertilized	After 50 years Effect of fertilization (B − A)	After 100 years C Unfertilized	After 100 years D Fertilized	After 100 years Effect of fertilization (D − C)
			High-latitude area fraction = 9.7%†			
Initialized at pre-industrial levels						
Our model	0	−26	−26	0	−39	−39
Peng and Broecker‡	—	—	—	0	−34	−34
Constant-emission	80	46	−34	156	98	−58
Business-as-usual	150	114	−36	430	362	−68
			High-latitude area fraction = 16.0%			
Initialized at pre-industrial levels	0	−41	−41	0	−59	−59
Constant-emission	79	24	−55	151	61	−90
Business-as-usual	146	88	−58	417	310	−107

* The scenario which is initialized at pre-industrial levels of atmospheric CO_2 has no anthropogenic source of CO_2 to the atmosphere, thus the CO_2 drawdown by the ocean results in a reduction below the initial pre-industrial value of 278.3 p.p.m. In the 'constant-emission' scenario, atmospheric CO_2 content is prescribed using observations until 1990[23], after which the CO_2 emission to the atmosphere is fixed at the model-determined value of 6.15 Gt C yr^{-1} in 1990. In the 'business-as-usual' scenario, the atmospheric CO_2 content is prescribed until 1989, after which the annual emission increases according to the IPCC business-as-usual scenario[22], in which the man-made emissions increase linearly with time from 6.0 Gt C yr^{-1} in 1990 to 22.4 Gt C yr^{-1} in 2100. The 1990 atmospheric CO_2 partial pressure is 355 p.p.m.

† The area fraction of 9.7% in our model corresponds to the same area in m^2 as chosen by Peng and Broecker[17].

‡ The Peng and Broecker[17] model is initialized at 280 p.p.m. and has a phosphate reduction of 1.6 mmol m^{-3}. The result given here is for their scenario with 17.5×10^6 m^{-3} s^{-2} of water upwelling in the high latitudes and being placed directly into the deep ocean.

enhanced carbon uptake resulting from iron fertilization. First is the reduction in average ΣCO_2 per unit area that occurs when fertilization is started. We take the supply of phosphate from depth as a reasonable guide to the maximum potential biological uptake of carbon, although we recognize that light supply, our ability to spread iron efficiently over the large ocean areas involved, the behaviour of the ocean ecosystem, and other processes may interfere long before the phosphate is depleted. (Carbon cycling is linked to that of phosphate through the Redfield ratio of C:P = 130 in organic matter.[18]) Second is the area over which the fertilization occurs. We use a recent analysis of National Oceanic Data Center phosphate data (S. Levitus and R. G. Najjar, personal communication) to estimate that the Southern Ocean's (>30° S) water volume in the depth range 0–75 m with phosphate ≥1.0 mmol m^{-3} amounts to 15.8% of the world ocean volume in the same depth range. The average phosphate content of this volume is 1.63 mmol m^{-3}. We therefore take the high-latitude box of our 'standard' model to consist of 16% of the world ocean area (with 9.7% as an alternative case corresponding to the area used by Peng and Broecker[17]), and we determine the enhancement to the biological production by forcing a reduction of phosphate by 1.5 mmol m^{-3} in the surface box of this area. Third is the reduction in CO_2 partial pressure resulting from a given carbon removal. We have found that this is considerably larger at high rather than at low CO_2 levels because of the nonlinear relation between P_{CO_2} and ΣCO_2. We use three different anthropogenic CO_2 emission scenarios to examine the contribution of this nonlinearity, one in which the ocean and atmosphere are initialized at the pre-industrial value of 278 p.p.m. with no anthropogenic sources, a 'constant-emission' scenario, and a 'business-as-usual' scenario (see Table 1 legend for descriptions of the scenarios).

The rate at which atmospheric CO_2 is taken up by the oceans also depends on the rate at which the ocean circulation and mixing transport to the abyss the excess CO_2 that invades the fertilized region from the atmosphere. As discussed below, we find that this factor is less critical than those mentioned above. Figure 1 shows the model we use to simulate the ocean circulation and mixing. Parameter values are obtained by fitting the model to pre-bomb ^{14}C observations as well as the GEOSECS bomb inventory estimates of Broecker *et al.*[19] (U.S. and F.J., to be published elsewhere). However, the bomb inventory estimates in the Southern Ocean were not considered adequate for use in the fitting exercise because the bomb signal is not easy to discern from the natural ^{14}C background; the data in the Southern Ocean are scanty, especially from pre-bomb time; and the bomb inventories south of 46° S show considerable variation. Instead, we checked our model with high-latitude CFC-11 observations, obtaining a standing crop of 1,976 nmol m^{-2} for 1984, comparable to an estimate of 1,950 ± 550 nmol m^{-2} obtained for the same period from measurements south of 46° S by Weiss *et al.*[20] in the South Atlantic, by the Pacific Marine Environmental Laboratory of the National Oceanic and Atmospheric Administration in the South Pacific (R. H. Gammon and D. Weisgarver, personal communication), and by R. Weiss (personal communication), also in the South Pacific.

Figure 2 summarizes results from the iron fertilization assuming the business-as-usual and constant-emission CO_2 scenarios. Without fertilization, the increase in atmospheric CO_2 from its 1990 value of 355 p.p.m. is 146 p.p.m. after 50 years, and 417 p.p.m. after 100 years in the business-as-usual scenario (Fig. 2*a*). When iron fertilization is initiated, an additional flux of organic carbon out of the high-latitude surface box is stimulated. Its size is approximately constant at 5.5 Gt C yr^{-1} after an initial peak in the first year. This increased carbon flux leads to a massive decrease in the high-latitude surface P_{CO_2} (see Fig. 2*b*), and a resulting enhancement of atmospheric CO_2 uptake so that the atmospheric CO_2 now increases by only 88 p.p.m. after 50 years (60% of the increase in the unfertilized scenario) and by 310 p.p.m. after 100 years (74% of the increase in the unfertilized scenario). The decrease in atmospheric P_{CO_2} resulting from iron fertilization reduces the low-latitude air–sea difference so that the response of the low latitude regions is opposite in sign to that of the high latitudes (Fig. 2*b*). After 100 years, the additional CO_2 flux from the atmosphere to the high-latitude box in the iron fertilization scenario is 2.65 Gt C yr^{-1}. This is partly balanced by a reduction of 0.51 Gt C yr^{-1} in the low-latitude uptake of anthropogenic CO_2, for a net annual oceanic uptake of 2.13 Gt C yr^{-1} due to iron fertilization.

The effect of the nonlinearity of the carbon chemistry equations can be discerned by comparing the three scenarios shown in Table 1. The constant-emission scenario with fertilization of 16% of the world ocean shows a reduction of 90 p.p.m. in the increase of atmospheric CO_2 resulting from 100 years of iron fertilization, compared with 59 p.p.m. for the scenario initialized at 278 p.p.m. The further increase in atmospheric CO_2 in the business-as-usual scenario has a still larger effect: 107 p.p.m. The dependence on the prevailing atmospheric CO_2

concentrations can be understood when considering that P_{CO_2} depends in a nonlinear way on ΣCO_2. The higher the atmospheric concentration of CO_2, the larger the change in oceanic P_{CO_2} for a given reduction of ΣCO_2 due to iron fertilization (see Fig. 2*c*). We find that the percentage reduction in atmospheric CO_2 concentration which would occur after 100 years of iron fertilization decreases with higher CO_2 levels (21% for pre-industrial initialization, 14% for the business-as-usual scenario). This is in contrast to the assertion of Peng and Broecker[17] that the relative reduction is constant.

Peng and Broecker[17] emphasize that the key to evaluating the impact of iron fertilization is the rate of vertical exchange in the Southern Ocean. We find that the uncertainty in the calibration of the high-latitude transport parameters u and w gives error limits of $^{+14\%}_{-24\%}$ for the absolute value of the iron-induced reduction in atmospheric CO_2 for the pre-industrial scenario. Therefore, the precise magnitude of the vertical exchange seems not to be as critical as uncertainties in other processes. This is also supported by the fact that Peng and Broecker's result agrees well with ours for the same pre-industrial scenario (Table 1), although their high-latitude vertical exchange, which is calibrated with bomb-produced radiocarbon, is considerably weaker than our vertical exchange calibrated by oceanic distribution of CFC-11.

The effect of ocean area is readily apparent from the results summarized in Table 1. An increase in the fertilized area from 9.7% to 16% leads to an almost linear increase in the effect of iron fertilization of ~60%. Broecker[21] argues that their choice of the smaller area was intended to compensate for the fact that much of the Antarctic is in darkness during part of the year. We attempted to compensate for this effect by fertilizing the ocean for only six months of the year. The CO_2 uptake in the business-as-usual case went down from 107 p.p.m. to 88 p.p.m. far less than the drop to 68 p.p.m. which occurs when using the smaller area.

To be effective, iron fertilization has to be applied continuously so that the atmosphere–ocean system does not revert to its unfertilized state. This is shown in Fig. 3, which shows what happens if iron fertilization is terminated after 50 years. At 50 years the ocean in the business-as-usual iron fertilization simulation has taken up 57.9 p.p.m. more CO_2 than the non-fertilized ocean. If fertilization is stopped at this point, the difference between the fertilized and non-fertilized scenarios reduces to 35.5 p.p.m. after 100 years.

Changes in the Earth's equilibrium temperature are logarithmically related to the atmospheric CO_2 content, with a doubling of CO_2 leading to an equilibrium warming of between 1.5 °C and 4.5 °C, with a preferred value of 2.5 °C (ref. 22). A useful index of the significance of a given CO_2 increase is the factor $\ln(P_{CO_2}/278)/\ln(2)$ which, multiplied by 2.5 °C, will give the equilibrium warming resulting from a given CO_2 increase. Thus, the atmospheric CO_2 concentration of 771 p.p.m. reached by 2090 in the business-as-usual scenario will give an equilibrium warming of 3.7 °C. The 107-p.p.m. additional oceanic uptake

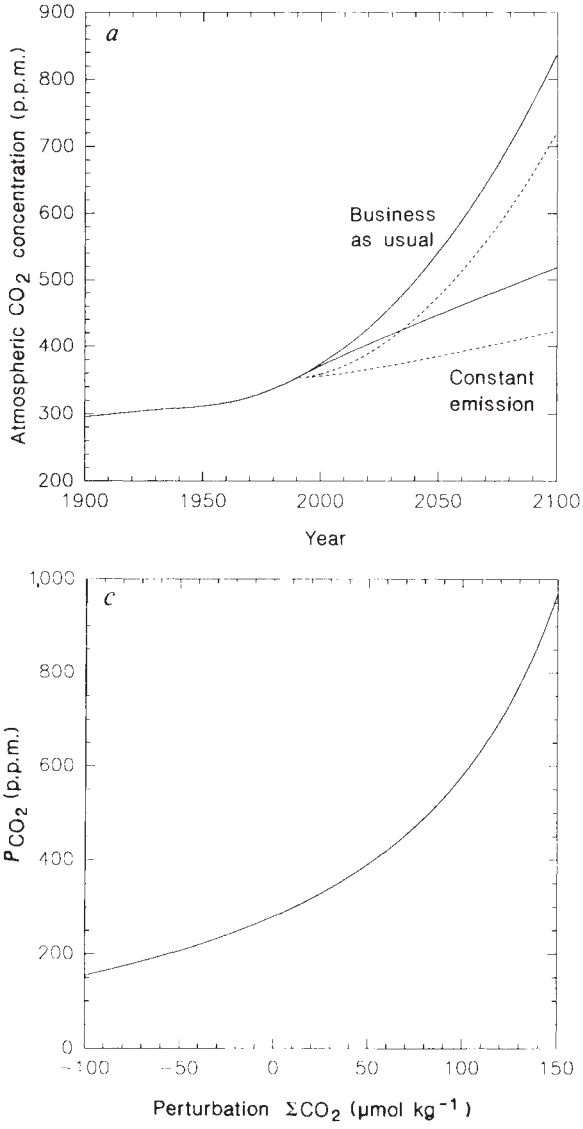

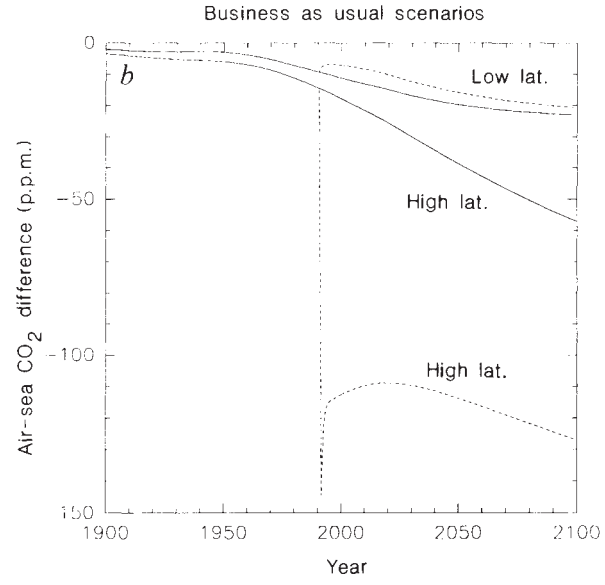

FIG. 2 *a*, Future atmospheric CO_2 concentration in the business-as-usual and constant-emission scenarios. The solid line is our prediction without iron fertilization, the dashed line shows what might occur with iron fertilization. *b*, The air–sea CO_2 difference of the iron-fertilized business-as-usual scenario (dashed lines) and the non-fertilized business-as-usual scenario (solid lines). *c*, Dependence of the partial pressure of CO_2 on ΣCO_2 in high-latitude surface water ($T = -0.22$ °C). With increasing CO_2 concentrations, the slope of the curve increases, and so does the change in P_{CO_2} for a given change in ΣCO_2.

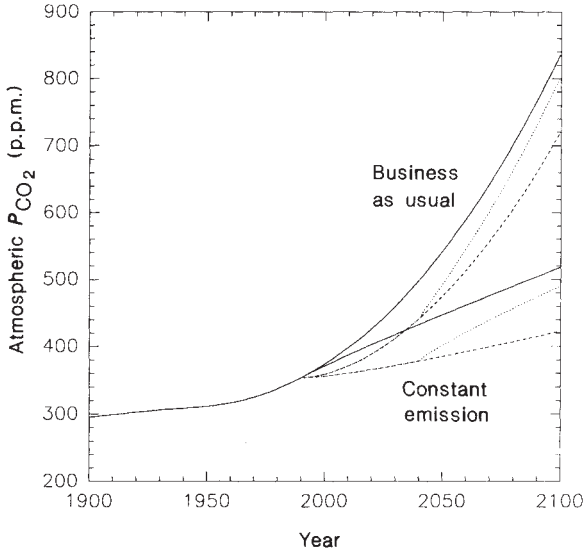

FIG. 3 The effect of stopping iron fertilization after 50 years (dotted line) is depicted for the business-as-usual and constant-emission scenarios. The solid line is the unfertilized scenario, the dashed line is the scenario for continuous fertilization.

resulting from iron fertilization gives an equilibrium warming of 3.1 °C instead. On the other hand, the unfertilized constant-emission scenario, which reaches 505 p.p.m. in 2090, gives a significantly smaller equilibrium warming of 2.2 °C, which is reduced to 1.4 °C with the 90 p.p.m. additional oceanic uptake resulting from iron fertilization. These numbers can be compared with the 0.9 °C equilibrium warming that can be expected from the present atmospheric CO_2 content of 355 p.p.m. It should be kept in mind that the transient warming is smaller than, and not necessarily proportional to the equilibrium warming, due primarily to the uptake of heat by the ocean.

The most important conclusion we draw from our calculations is that, although the effect of iron fertilization is large enough to justify further study, the effect of a significant change in the emissions of CO_2 is even larger. We emphasize the preliminary nature of our calculations and the fact that all the assumptions we have made have been biased so as to yield an upper limit. □

Received 5 November 1990; accepted 5 February 1991.

1. Booth, W. *Washington Post*, A1 20 May (1990).
2. Baum, R. *Chem. Engng News* **68,** 21–24 (1990).
3. Martin, J. H., Fitzwater, S. E. & Gordon, R. M. *Global biogeochem. Cycles* **4,** 5–12 (1990).
4. Knox, F. & McElroy, M. B. *J. geophys. Res.* **84,** 2503–2518 (1984).
5. Siegenthaler, U. & Wenk, T. *Nature* **308,** 624–626 (1984).
6. Sarmiento, J. L. & Toggweiler, J. R. *Nature* **308,** 621–624 (1984).
7. Sarmiento, J. L., Toggweiler, J. R. & Najjar, R. *Phil. Trans. R. Soc.* **A325,** 3–21 (1988).
8. Martin, J. H. & Fitzwater, S. E. *Nature* **331,** 341–343 (1988).
9. Martin, J. H. & Gordon, R. M. *Deep-Sea Res.* **35,** 177–196 (1988).
10. Martin J. H., Gordon, R. M., Fitzwater, S. & Broenkow, W. W. *Deep-Sea Res.* **36,** 649–680 (1989).
11. Martin, J. H. *Paleoceanography* **5,** 1–13 (1990).
12. de Baar, H. J. W. *et al. Mar. Ecol. Prog. Ser.* **65,** 105–122 (1990).
13. Banse, K. *Limnol. Oceanogr.* **35,** 772–775 (1990).
14. Dugdale, R. C., & Wilkerson, F. P. *Global biogeochem. Cycles* **4,** 13–20 (1990).
15. Anderson, G. C. & Morel, F. M. M. *Limnol. Oceanogr.* **27,** 789–813 (1982).
16. Morel, F. M., & Hudson, R. J. in *Chemical Processes in Lakes* (ed. Stumm, W.) 251–270 (Wiley, New York, 1985).
17. Peng, T.-H. & Broecker, W. S. *Nature* **349,** 227–229 (1991).
18. Toggweiler, J. R. & Sarmiento, J. L. in *The Carbon Cycle and Atmospheric CO_2: Natural variations Archean to Present* Vol. 32, Geophysical Monograph Series (eds. Sundquist, E. T. & Broecker, W. S.) 163–184 (American Geophysical Union, Washington, DC. 1985).
19. Broecker, W. S. Peng, T.-H., Östlund, G. & Stuiver, M. *J. geophys Res.* **90,** 6953–6970 (1985).
20. Weiss, R. F., Bullister, J. L., Warner, M. J., Van Woy, F. A. & Salameh, P. K. *Ajax Expedition Chlorofluorcarbon Measurements* (Scripps Institution of Oceanography Reference 90–6, La Jolla, 1990).
21. Broecker, W. S. *Global biogeochem. Cycles* **4,** 1–2 (1990).
22. Houghton, J. T., Jenkins, G. J. & Ephraums, J. J. (eds) *Climate Change*, The IPCC Scientific Assessment (Cambridg, University Press, 1990).
23. Siegenthaler, U. & Oeschger, H. *Tellus* **39B,** 140–154 (1987).
24. Peng, T. H., Takashi T. & Broecker, W. S. *Tellus* **39B,** 439–458 (1987).

ACKNOWLEDGEMENTS. We appreciate the great help given to F.J. by M. Warner in setting up our CFC runs, and his generosity and that of R. Gammon in helping us to obtain the CFC data needed to estimate the CFC inventories. R. Fink developed our carbonate system algorithm and R. Slater helped with the phosphate data analysis. J. R. Toggweiler and J. Orr provided helpful comments on the manuscript. F.J. and U.S. acknowledge the hospitality of the Atmospheric and Oceanic Sciences Program during their extended visit to Princeton. This work was funded by subcontracts with Martin Marietta Systems, Inc., under contract with the Carbon Dioxide Research Division, US Department of Energy; by a follow-up contract directly from the Carbon Dioxide Research Division of the Department of Energy; and by the National Science Foundation.

Biases from natural sulphurization in palaeoenvironmental reconstruction based on hydrocarbon biomarker distributions

Math E. L. Kohnen, Jaap S. Sinninghe Damsté & Jan W. De Leeuw

Organic Geochemistry Unit, Faculty of Chemical Technology and Materials Science, Delft University of Technology, De Vries van Heystplantsoen 2, 2628 RZ Delft, The Netherlands

BIOMARKERS (chemical fossils) are sedimentary organic compounds whose basic skeletons suggest an unambiguous link with known contemporary natural products, and were synthesized by biota present at the time of the deposition of the sediment. These compounds are commonly used to assess palaeoenvironmental conditions of deposition of Recent and ancient sediments[1–3]. Saturated hydrocarbons are relatively easy to analyse and contain a lot of geochemical information, and are therefore the most widely used class of biomarkers in palaeoenvironmental reconstruction[2–5]. Hydrocarbon biomarkers are biosynthesized as such or are derived from functionalized biosynthetic lipids, such as alkenes, alcohols and acids, by diagenetically induced defunctionalization. Functionalized lipids may, however, also undergo an abiogenic reaction with hydrogen sulphide or polysulphides ('natural sulphurization') during the early stages of diagenesis, and this may lead to selective removal of specific hydrocarbon biomarker precursors. Here we investigate the influence of natural sulphurization on hydrocarbon biomarker signatures in immature sediments from Italy and off Peru. We show that, if not taken properly into account, this process may lead to a severe bias in the interpretation of the geological record.

Sedimentary functionalized lipids react with reduced sulphur species (H_2S and HS_x^-) to form organic sulphur compounds (OSCs) and sulphur-bound lipid moieties in macromolecules (see ref. 6 for a review). The onset of sulphurization of organic matter is controlled by the reactive iron (for example, ferrihydrite and haematite) content of the sediment, because organic matter reacts with reduced sulphur more slowly than do sedimented iron minerals and thus does so only after reactive iron oxides have first been converted to iron sulphides. In the region of upwelling in the Peru margin, sulphur incorporation into sedimentary organic matter starts in the top metre of the sediment column[7], indicating that this process occurs in the early stages of diagenesis. Moreover, the identification of OSCs in a Recent Black Sea sediment (age $3–6 \times 10^3$ yr) also points to an early diagenetic sulphurization of organic matter[8]. Ten Haven *et al.*[9] examined the extracts of almost 100 thermally immature deep-sea sediments and found that approximately 70% of the samples contain OSCs. The widespread occurrence of OSCs, and the fact that reduced inorganic sulphur species are present in any anoxic organic-matter-containing Recent marine sediment[10], suggest that natural sulphurization of specific functionalized lipids is a ubiquitous process. It seems inevitable that this selective removal of the precursors of hydrocarbon biomarkers will alter the hydrocarbon biomarker distribution in immature sediments, and thus the interpretation of the geological record as revealed by their apparent distribution. Hydrocarbon biomarkers are used in many (palaeo)environmental reconstruction studies of immature sediments[11–16] and of par-